

Received January 25, 2022, accepted February 22, 2022, date of publication February 25, 2022, date of current version March 4, 2022.

Digital Object Identifier 10.1109/ACCESS.2022.3154765

Joint Iterative Blind Self-Interference Cancellation, Propagation Channel Estimation and Decoding Processes in Full-Duplex Transmissions

BAO QUOC VUONG^{1,2,3}, (Graduate Student Member, IEEE),
ROLAND GAUTIER¹, (Member, IEEE), **ANTHONY FICHE**¹, (Member, IEEE),
MÉLANIE MARAZIN¹, (Member, IEEE), **HIEN QUANG TA**^{2,3}, (Member, IEEE),
AND LAP LUAT NGUYEN^{2,3}, (Member, IEEE)

¹Lab-STICC, CNRS, UMR 6285, University of Brest, 29200 Brest, France

²School of Electrical Engineering, International University, Ho Chi Minh City 700000, Vietnam

³Vietnam National University, Ho Chi Minh City 700000, Vietnam

Corresponding author: Bao Quoc Vuong (bao.vuong@univ-brest.fr)

This work was supported in part by the Brest Institute of Computer Science and Mathematics (IBNM), CyberIoT Chair of Excellence at the University of Brest (UBO); in part by the Brittany Region-Pôle d'Excellence Cyber; and in part by the UBO Grant "Ph.D. Student International Mobility" of Direction Europe and International (DEI) for 3 Months Mobility in International University, Vietnam National University, Ho Chi Minh City, Vietnam.

ABSTRACT The paper proposes a joint blind iterative Self-Interference (SI) cancellation, propagation channel estimation and decoding algorithm in Full-Duplex (FD) transmissions via feedback of channel estimates and decoded messages combined with the process of Digital Self-Interference Cancellation (DSIC). Different from the conventional algorithm, the proposed blind algorithm simultaneously estimates the self-interference and propagation channels and decodes messages in each decoding iteration of 5G Quasi-Cyclic Low Density Parity Check (QC-LDPC) codes. The temporary propagation channel estimate and decoded message are fed back to improve the self-interference cancellation and also the channel estimation as well as decoding in the next iteration. The results show that the proposed algorithm outperforms the conventional algorithm, especially at high signal to noise ratio (SNR) and small number of symbols, and requires much less processing time and computational complexity while achieving the convergence performance. The results also show that the proposed algorithm is less sensitive to SI level than the conventional algorithm. The paper further proposes a partial feedback scheme, which only use few feedback symbols for channel estimation, to significantly reduce the processing time and computational complexity while maintaining the performance. These good properties seem quite suitable for a use of this proposed blind iterative algorithm for short-length packet FD transmissions in Internet-of-Things (IoT) applications and green communications.

INDEX TERMS Full-duplex, digital self-interference cancellation, 5G QC-LDPC codes, short-packet transmission, blind channel estimation, iterative channel estimation and decoding.

I. INTRODUCTION

In the era of 5G wireless communications, associated with Internet-of-Things (IoT) support, in order to enable many new devices to communicate and to be able to make autonomous decision by deploying diverse technologies and

The associate editor coordinating the review of this manuscript and approving it for publication was Wei Feng.

connecting massive devices [1]–[3]: two main services are targeting which are ultra-Reliable Low-Latency communications (uRLLC) and massive Machine-Type Communications (mMTC) [4]. The uRLLC strictly requires reliability and latency, since it concentrates on supporting mission-critical applications such as intelligent transportation and industry automation [2], [5]. The mMTC brings advantages on energy efficiency, since it concentrates on supporting

massive machine-type applications which can be up to thousands of devices such as wearable or smart applications and sensors in IoT [6]. In order to be efficient, both uRLLC and mMTC require the use of short-length information frame, and certainly provide short-packet transmissions in their applications. Moreover, the implementation of physical-layer security for both uRLLC and mMTC lead to promote even more the use of short-length packets transmissions [1]. Short-length packet transmission is considered as a fundamental of security in 5G and IoT applications compared to the normal packet transmission system in order to ensure robustness with respect to interception (eavesdropper) or jamming [7].

An increasing number of IoT devices leads to an issue of spectrum shortages, which requires emerging techniques to share the spectrum efficiently. Full-Duplex (FD), simultaneously transmitting and receiving information through the same channel, is a promising technique for 5G & Beyond wireless networks as it can double “theoretically” the spectral efficiency, compared to the traditional Half-Duplex (HD) [8]. Unfortunately, in practice for this FD transmission scheme, a Self-Interference (SI) problem appears caused by the significant difference between the power of the useful signal received and the power of the signal emitted by the transmitting antennas very close to that of reception and which then strongly disturbs the reception [9]. So, SI cancellation would play the most important role in implementing FD communication systems in both academia [10], [11] and industry [12], [13]. Therefore, this SI must be suppressed close to the noise floor level, otherwise the spectral efficiency will be impaired due to the high level of interference. Nevertheless, it is indisputable that FD transmission schemes can bring many advantages to modern wireless communications systems, both in terms of spectral efficiency but also security through the use of self-jamming techniques (covert communications). To overcome the SI problem, various approaches have been proposed such as passive technique with Radio Frequency (RF) cancellation (beamforming, antenna decoupling or isolation, cross-polarization, ...) [14]–[16], or active techniques with analog cancellation [17], [18] (analog filter, ...) and digital cancellation [19].

Assuming that interference cancellation steps are already implemented at the RF and analog level with acceptable performance (what is outside the scope of this study, but essential in practice), the residual SI channel can be estimated by using Digital Self-Interference Cancellation (DSIC) process based on Least Mean Square (LMS), Normalized Least Mean Squared (NLMS) or Recursive Least Square (RLS) algorithms [19]. Since the SI component is created by the transmitter itself, it can be used to successfully cancel the residual SI from the received signal to retrieve the signal of interest. Then, an equalizer (Decision Feedback Equalizer (DFE), linear equalizer, ...) is applied to estimate the channel of interest and detect the desired data. Traditionally, these processes work independently and thus, the problem of time consumption and quality of transmission have not been adapted in case of short-frame transmission.

The DSIC requires more processing steps at the receiver and assumption on the signal knowledge and SI channels have to be done to perform the blind or semi blind estimations [20]–[23]. Particularly, joint algorithms channel estimation are proposed, for instance, as in [24]. With an iterative Maximum Likelihood (ML) channel estimator for both SI and intended (propagation) channels can be estimated by taking into account the known SI, the pilots and unknown data symbols of the signal. However, the performance is significantly degraded in short-frame communication because of the consecutive pilot transmission for a long period. In [25], the joint estimate coefficients of both SI, intended channels and transceiver impairments have been proposed by using subspace algorithm. Nevertheless, the results in short-frame communication are still in expectation because it needs more data symbols to obtain a good second-order statistics of received signal. So, it is still not a satisfying solution for time, bandwidth and power efficient approaches for short-frame transmission in FD transmission. This issue is a constraint since it requires a large number of pilot symbols to obtain the saturation of channel estimation. Therefore, the short length of pilot symbols for channel estimation in short-frame communications receives a lot of concerns. Furthermore, the use of FD short-packet transmission has also been faced with some drawbacks such as high estimation error of the SI channel [26] as well as the high latency of decoding process, i.e. in 5G Quasi-Cyclic Low Density Parity Check (QC-LDPC) decoder [27], [28], because the decoder uses a lot of iterations to achieve the convergence or saturation level. These challenges of the FD short-frame transmission still receive a lot of interests of researchers in recent years.

In this paper, we investigate joint iterative channel estimation and decoding algorithms in FD transmissions in the digital domain via feedback of channel estimates and decoded messages combined with the process of DSIC. The first algorithm is a blind version. The idea is to repeat the simultaneous process of channel estimation and decoding with the DSIC process via feedback to minimize the error of channel estimates and decoded messages. The intended message is temporarily decoded from the received signal and later is re-encoded, re-modulated, re-interleaved and fed back to the process per each 5G QC-LDPC decoding iteration. After some iterations for a sufficient saturation, the channel estimates and decoded messages can be achieved with the minimum error. The channel estimation processes for both SI channel and intended channel are based on the RLS algorithm as its best performance with faster convergence compared to others [29]–[31]. It is used to monitor the change in time of the SI channel per each iteration to get a better estimation and reconstruction of the interference and intended signals. Firstly, we illustrate the influence of the proposed algorithm in both SI and intended channel estimations. Then, the system performance such as mean square error, bit-error-rate and processing time will be illustrated for the proposed and conventional algorithms. Furthermore, a partial feedback scheme

is considered to reduce the processing time of the proposed blind algorithm.

Throughout the paper, the performance evaluation of the proposed algorithms is based on three metrics: Mean Square Error (MSE), Bit-Error-Rate (BER), processing time and computational complexity. The contributions of this paper can be summarized as follow:

- We propose a joint iterative *blind* channel estimation and decoding for short-frame transmissions;
- We characterize the out-performance of the system with feedback using the proposed algorithm compared to that without feedback;
- We point out that the number of joint iterations in the proposed algorithms with the use of 5G QC-LDPC codes is required only four iterations to achieve the convergence performance;
- We further propose a partial feedback scheme which only use a partial number of modulated symbols in feedback loop for channel estimation processes and it can significantly reduce the processing time and computational complexity while maintaining the convergence performance;

The remaining of this paper is organized as follows. Section II describes briefly the system model of FD transmissions, the 5G QC-LDPC codes and the conventional DSIC algorithm. Section III proposes the joint iterative *blind* channel estimation and decoding algorithm with numerical results and comparisons with the conventional algorithm. Section IV introduces the partial feedback scheme and compares the processing time and computational complexity of all schemes. Finally, some highlights and conclusions will be discussed in section V. The notations in this paper are summarized in Table 1.

TABLE 1. List of Notations.

Notations	Meaning
K	Information length
N	Code word length
R	Code rate
M	Modulation order
E	Frame length after modulation
α	Partial feedback coefficient
\mathbf{h}_{XY}	Channel gain vector between X and Y
\mathbf{h}_{XX}	Self-interference channel gain vector
$v[k]$	k -th bit of signal vector \mathbf{v} in bit domain
$v[n]$	n -th symbols of signal vector \mathbf{v} in discrete time domain
$v(t)$	Signal \mathbf{v} in continuous time domain
$\hat{\mathbf{v}}$	Estimation value of \mathbf{v}
$\tilde{\mathbf{v}}$	Residual value of \mathbf{v}
$*$	Convolution operator
λ	Forget factor of RLS algorithm
i	Index of joint iterative iterations
j	Index of 5G QC-LDPC decoding iterations
d_v	Average degree of the variable nodes
d_c	Average degree of the check nodes

II. SYSTEM MODEL

We consider a Single Input Single Output (SISO) short-packet transmissions between two nodes, A and B, which

are equipped with two antennas for simultaneously transmitting and receiving messages in FD modes as showed in Fig. 1. Assuming that 5G QC-LDPC codes for both uplink and downlink short-packet transmissions [32], are used at transceivers. We also assume that the channel gains between two nodes and the SI channel gains at each node itself are denoted \mathbf{h}_{XY} and \mathbf{h}_{XX} , respectively, where $X, Y \in \{A, B\}$, and \mathbf{h}_{XY} and \mathbf{h}_{XX} are i.i.d complex Gaussian random variables with mean 0 and variance 1. In general, the SI channel of FD transmissions consists of two components: Line-of-Sight (LoS) and Non Line-of-Sight (NLoS). By using passive suppression techniques, the LoS component can be mitigated significantly while the reflections is mitigated slightly [19]. This leads to the interference channel reasonably modeled as Rayleigh fading in digital domain.

Due to the symmetric property at each node in FD transmissions, the channel estimation and decoding performance will be the same at each node. Without loss of generality, we consider signal at node A side and its received signal in time domain can be given by:

$$y(t) = y_{SI}(t) + y_{BA}(t) + w(t), \quad (1)$$

where $y_{SI}(t)$ is the self-interference component consisting of the SI signal \mathbf{x}_{SI} ¹ passing through the SI channel \mathbf{h}_{AA} and $y_{BA}(t)$ is the received intending component consisting of the intended signal \mathbf{x}_B passing through the propagation channel \mathbf{h}_{BA} . Therefore, Equation (1) can be expressed as:

$$y(t) = (\mathbf{h}_{AA} * \mathbf{x}_{SI})(t) + (\mathbf{h}_{BA} * \mathbf{x}_B)(t) + w(t). \quad (2)$$

The operator $(*)$ denotes the convolution and $w(t)$ is the complex Gaussian noise with mean 0 and variance σ_w^2 .

Next, we will briefly mention 5G QC-LDPC codes for $x_{SI}[k]$ and $x_B[k]$, and the conventional algorithm, named the *DSICED3_W/O/F scheme*, for Digital Self-Interference Cancellation, Equalization, Demodulation, De-interleaving and Decoding Without Feedback scheme.

A. 5G QC-LDPC CODES

The classical LDPC codes was first proposed by Gallager in 1962 [33] and rediscovered again by MacKay in the late 1990s [34]. Based on the properties and characteristics of classical LDPC codes, a new version named QC-LDPC has been considered by the 3GPP for 5G networks and applications. It is considered as the standard codes of 5G for the control information in uplink and downlink because they support a number of lifting size and different code rate with high throughput and low latency [32]. It can be also considered as a candidate in 5G channel coding scheme for short length frame with lower processing throughput for the mMTC or massive Machine to Machine (mM2M) [27]. Furthermore, 5G QC-LDPC codes is also an optimized design for short-packet transmission with low error floor and high speed transmission [35]–[37]. The Base Graph (BG) matrix and

¹The transmitted signal at node A is denoted by \mathbf{x}_{SI} rather than \mathbf{x}_A in order to distinguish the SI and the intended signal.

exponent parity check matrix \mathbf{H} are the basic fundamental to construct the 5G QC-LDPC codes, which are described in detail in [32], [38], [39]. At the transmitting side, the (N, K) 5G LDPC encoding process, between the exponent parity check matrix \mathbf{H} and the information bit sequence is based on Gauss-Jordan elimination algorithm [40], where N and K denote the code word length and information length, respectively. While at the receiving side, the Sum Product Algorithm (SPA) decoding algorithm with an efficient message passing schedule will be implemented in the 5G LDPC decoding process [41], [42], where the check node and the symbol node do the iterative decoding by sending message that carry their guesses of code word bits to each other for each decoding iteration j , until it achieved the maximum number of interactions j_{max} . The Log Likelihood Ratio (LLR) is used to reduce the complexity of computation because the SPA involves a lot of multiplications and using LLR results in the replacement of these by summations in log-domain. At the end of each iteration, a hard decision is applied to obtain the estimated input bit sequence.

B. CONVENTIONAL DSICED3 W/OF SCHEME

In this subsection, we describe the Digital Self-Interference Cancellation, Equalization, Demodulation, De-interleaving and Decoding Without Feedback scheme and the signal processing of both transmitting and receiving side. The general SISO FD transmission model between two nodes A and B in the presence of channel coding scheme, DAC/ADC process is described in Fig. 1. At the transmitting side, the input information message sequence $x_{SI}[k]$ in bit domain, where $k \in [1, K]$, will be encoded by using (N, K) 5G QC-LDPC codes, to form a codeword with length N . Then, this codeword sequence is interleaved, modulated with QPSK modulator by modulation order $M = 4$ to form a complex symbol sequence $x_{SI}[n]$, where $n \in [1, E]$ and $E = N/\log_2(M)$. After that, it is converted to continuous time domain by DAC process to form the transmitted signal $x_{SI}(t)$ and to be passed to RF for being transmitted to node B. The same process is applied at node B for $x_B(t)$.

At the receiving side, node A receives summation signal and then passes it to the ADC process for being converted to the discrete time domain signal, $y[n]$. Here, the bit resolution and voltage dynamic range of DAC/ADC architecture should be chosen highly enough to avoid the residual quantization noise error, which has been studied in [43]. In this paper, the impacts of DAC/ADC, other hardware impairments on the SI cancellation and the synchronization problem between the signals are not considered (which is outside of this study but essential for practice). Then, DSIC process is applied to obtain the estimated SI channel $\hat{\mathbf{h}}_{AA}$ by using an adaptive filter with RLS algorithm. Here, the forgetting factor λ of RLS algorithm should be chosen between 0.9 and 1 [44]. Since node A knows its transmitted signal $x_{SI}[n]$, a copy version of $x_{SI}[n]$ can be used to eliminate the SI component to obtain:

$$\tilde{y}[n] = y[n] - \hat{y}_{SI}[n] = y[n] - (\hat{\mathbf{h}}_{AA} * \mathbf{x}_{SI})[n]. \quad (3)$$

Then, the binary output $\hat{x}_{SI}[k]$ of the signal of interest can be obtained from $\tilde{y}[n]$ via equalization, demodulation, de-interleaving and decoding processes. In the decoding, the LLR belief sequence that received from the soft remapping QPSK demodulation process will be used for decisions and the SPA decoding algorithm is performed [41], [42]. To reconstruct the intended binary input signal $\hat{x}_{SI}[k]$ of node B, we use the SPA at node A, i.e. the message passing between the check nodes and the symbol nodes for guessing the transmitted bits from each other at each iteration j until it reaches the maximum number of interactions j_{max} .

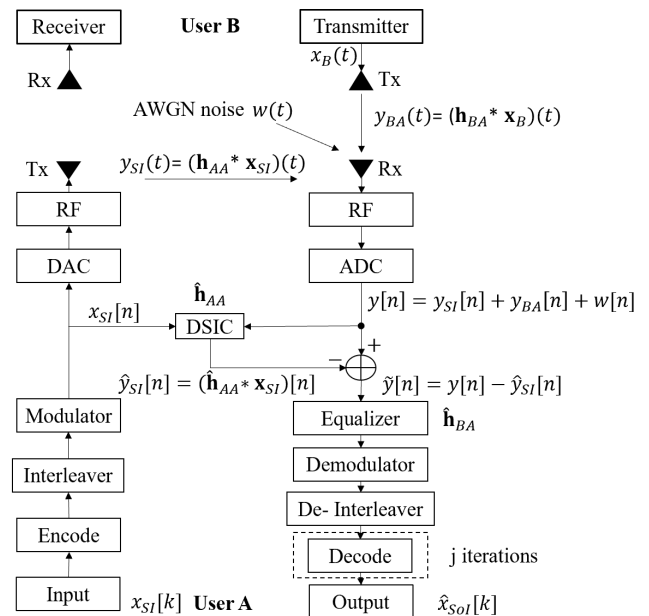


FIGURE 1. SISO FD transmission with DSICED3 W/OF process.

III. PROPOSED JOINT ITERATIVE BLIND SCHEME

The conventional DSICED3_W/OF scheme requires LLR sequence and decoding updated per iteration after channels are estimated and the SI is cancelled, which means that the channel estimations and the SI cancellations are separated from the decoding process. This leads to some drawbacks of this conventional scheme such as high estimation error of the SI channel [26] as well as the high latency of 5G QC-LDPC decoder [27], [28] in short-packet transmissions. To overcome these drawbacks, the channel estimations and the SI cancellations should be embedded into the iterative process of decoding to obtain a novel scheme, that we name JIB_DSICED3 for Joint Iterative Blind Digital Self-Interference Cancellation, Equalization, Demodulation, De-interleaving and Decoding scheme.

The JIB_DSICED3 scheme is depicted in Fig. 2, in which the proposed scheme is developed on the principle that the processes of SI cancellation and decoding of the desired signal can benefit from each other via the temporary decoding and feedback loop after each joint iteration decoding i , where $i \in [1, i_{max}]$. We emphasize that, different from the iteration j

performing the iteration decoding in the system without feedback in Section II-B, the iteration i in the proposed algorithm is for the joint channel estimation and decoding via feedback. We also emphasize that including many j iterations decoding into each of i iterations in the JIB_DSICED3 scheme will increase latency and complexity because the SPA decoding process between the check node and variable nodes is an optimal iterative decoding algorithm, but with high computational complexity [45]. Hence, the proposed scheme will only consider one iteration decoding ($j = 1$) for each joint iteration i , called temporary decoding, and later, it will be proved that the proposed scheme requires only a few iterations to achieve a saturation performance. The proposed iterative algorithm are presented in the following four main steps:

Step 1: SI channel estimation and DSIC process

First of all, a copy version of the transmitted signal $x_{SI}[n]$ in digital domain and the received signal at the receiver of node A after ADC process $y[n]$ are used to calculate the error signal in DSIC process. Then based on this error, we can control and modify the unknown SI channel vector $\hat{\mathbf{h}}_{AA}$ by using adaptive filter with RLS algorithm. As a result, we can effectively obtain the estimation of the SI channel and achieve the interference component $\hat{y}_{SI}[n]$. The output signal after this step can be express as:

$$\tilde{y}^{(i)}[n] = y[n] - \hat{y}_{SI}^{(i)}[n] = y[n] - (\hat{\mathbf{h}}_{AA}^{(i)} * \mathbf{x}_{SI})[n]. \quad (4)$$

Step 2: Intended channel estimation

The residual signal $\tilde{y}^{(i)}[n]$ received from Step 1 will pass through an equalizer with RLS algorithm in order to firstly estimate the intended multi-path fading channel $\hat{\mathbf{h}}_{BA}$ and then obtain the equalized signal with reducing of the effects of multi-path fading channel and AWGN noise. Here, a *blind* channel estimation method with RLS algorithm is applied with no knowledge from the transmitting signal from node B, where the initial value of $\mathbf{x}_B^{(0)} = \mathbf{0}$ when starting the iterative process. Then, the equalized signal continues to go to the QPSK demodulator and de-interleaver process to get the LLR belief information sequence for decoding.

Step 3: Decoding of the intended signal

Then, the temporary estimation of binary intended signal of node B $\hat{x}_{Sol}^{(i)}[k]$ is achieved by using 5G QC-LDPC decoding process with the exchange belief information between the variable nodes and check nodes as Section II-A for each iteration. In this step, only one SPA decoding iteration is used ($j_{max} = 1$).

Step 4: Feedback loop

When the temporary binary data of the intended signal is estimated and the maximum number of joint iteration i_{max} is not reached, it goes to the feedback loop with re-encoding, re-interleaving, and re-modulation processes to obtain the feedback signal $\hat{x}_B^{(i)}[n]$. This signal will take a convolution process with the estimation version of the intended channel

Algorithm 1: Proposed Joint Iterative Blind Scheme

```

Inputs :  $\mathbf{y}, \mathbf{x}_{SI}, i_{max}, K, N, M;$ 
Outputs :  $\hat{\mathbf{h}}_{AA}^{(i_{max})}, \hat{\mathbf{h}}_{BA}^{(i_{max})}, \mathbf{x}_{Sol}^{(i_{max})};$ 
Initialization:  $\hat{\mathbf{y}}_{BA}^{(0)} = \mathbf{0}, \hat{\mathbf{h}}_{AA}^{(0)} = \mathbf{0}, \hat{\mathbf{h}}_{BA}^{(0)} = \mathbf{0}, \mathbf{x}_B^{(0)} = \mathbf{0};$ 
for  $i = 1$  to  $i_{max}$  do
    /* Perform all steps for all of  $E$ 
    symbols, with  $E = N/\log_2(M)$ ,  $N$  is
    code word length,  $M$  is modulation
    order */
    for  $n = 1$  to  $E$  do
        Step 1: SI channel estimation and DSIC process
        Estimate:  $\hat{\mathbf{h}}_{AA}^{(i)}$ ;
        Calculate:
         $\tilde{y}^{(i)}[n] = y[n] - \hat{y}_{SI}^{(i)}[n] = y[n] - (\hat{\mathbf{h}}_{AA}^{(i)} * \mathbf{x}_{SI})[n];$ 
        Step 2: Intended channel estimation
        Estimate:  $\hat{\mathbf{h}}_{BA}^{(i)}$  and calculate LLR belief sequence of
         $\mathbf{x}_{Sol}^{(i)}$ ;
    end
    /* Decoding for all  $K$  symbols */
    for  $k = 1$  to  $K$  do
        Step 3: Decoding of the intended signal
        Decoding:  $\hat{x}_{Sol}^{(i)}[k];$ 
    end
    if  $i < i_{max}$  then
        /* Perform Step 4 for all  $E$  symbols
        */
        for  $n = 1$  to  $E$  do
            Step 4: Feedback loop
            Perform feedback loop to get  $\hat{x}_B^{(i)}[n];$ 
            Calculate:  $\hat{y}_{BA}^{(i)}[n] = (\hat{\mathbf{h}}_{BA}^{(i)} * \hat{\mathbf{x}}_B^{(i)})[n];$ 
            Update:  $y_{DSIC}^{(i+1)}[n] = y[n] - \hat{y}_{BA}^{(i)}[n];$ 
        end
    else
        /* It is the end of the processing
        of this algorithm */
        Go to return
    end
end
return  $\hat{\mathbf{h}}_{AA}^{(i_{max})}, \hat{\mathbf{h}}_{BA}^{(i_{max})}, \mathbf{x}_{Sol}^{(i_{max})}.$ 

```

$\hat{\mathbf{h}}_{BA}^{(i)}$, which is obtained in Step 2, to form the feedback intended signal as $\hat{y}_{BA}^{(i)}[n] = (\hat{\mathbf{h}}_{BA}^{(i)} * \hat{\mathbf{x}}_B^{(i)})[n]$. As can be seen from Equation (1), the received signal is the combination of the SI signal, intended signal and AWGN. Consequently, the feedback intended signal $\hat{y}_{BA}^{(i)}[n]$ is used to remove temporarily the intended component in order to optimize the SI channel estimation process for the next decoding iteration. It is given by:

$$y_{DSIC}^{(i+1)}[n] = y[n] - \hat{y}_{BA}^{(i)}[n]. \quad (5)$$

The proposed algorithm can be summarized in Algorithm 1. The most important metrics in channel estimation performance, MSE and BER under the two cases with and without feedback will be computed by using Monte Carlo simulations on MATLAB. For 5G QC-LDPC codes, the base graph matrix **BG2** is implemented for all simulations. The number of joint iteration with feedback and 5G LDPC codes decoding are

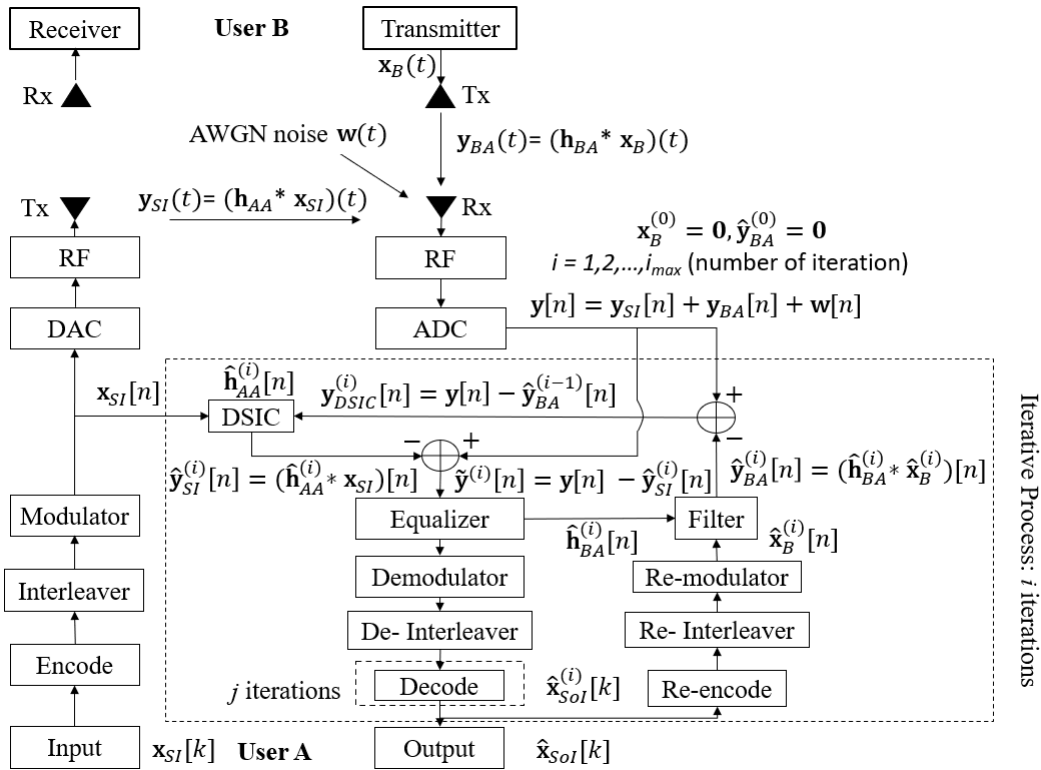


FIGURE 2. SISO FD transmission with proposed JIB_DSICED3 process.

denoted as i and j , respectively. Many simulation tests have been implemented with different channel models and number of channel taps (range from 3 to 8 taps). The changing of channel does not change the performance results very significantly. Because of the limitation and not to overload the paper, all of the configurations and figures are not provided for reasons of readability of the paper and better understanding. Therefore, the SI channel is fixed with 3 taps while the intended channel is fixed with 4 taps according to the ITU-R Pedestrian test environment channel model [46]. These channels are generated independently in each transmission frame. The simulation parameters are summarized in Table 2.

TABLE 2. Simulation Specifications.

Parameter	Value
Codeword length (N)	256
Information length (K)	128
Code rate (R)	1/2
Number of transmission frames	1000000
Modulation scheme (M)	QPSK ($M = 4$)
SI channel taps	3
Intended channel taps	4
Forget factor λ	0.999

Next, we will characterize the performance of the proposed scheme JIB_DSICED3 and compared to that of the conventional scheme DSICED3_W/OF in terms of MSE, BER and processing time.

A. MSE PERFORMANCES: JIB_DSICED3 VS DSICED3_W/OF

In this subsection, we also introduce a particular scheme called Best Performance Scheme (BPS), corresponding to a lower bound (but not realistic in practice) using the proposed JIB_DSICED3 scheme with considering that all of intended E symbols from user B are known, as a benchmark to characterize the optimality of the proposed JIB_DSICED3 scheme in terms of MSE and for performance comparison. Indeed, in this limit case, the system does not need to perform the temporary decoding in step 3 and re-encoding, re-interleaving and re-modulation processes in step 4. Instead, in step 4, it only considers using all known E symbols to do a filter process with the estimation version of intended channel \hat{h}_{BA} in step 2 to obtain the estimation version of intended signal \hat{y}_{BA} for subtraction in the next iterations.

The MSE of the SI channel and the intended channel are respectively given by, [24].

$$MSE_{SI} = |h_{AA} - \hat{h}_{AA}^{(i)}|^2, \tag{6}$$

$$MSE_{BA} = |h_{BA} - \hat{h}_{BA}^{(i)}|^2. \tag{7}$$

Fig. 3 and Fig. 4 show the MSE in decibel (dB) scale of the SI signal and the intended channel versus number of modulated symbols E for various values of number of decoding iterations, respectively. Based on the background noise as the reference, the self-interference to noise ratio, p_{SI}/σ_w^2 and the SNR, p_B/σ_w^2 are set up at 30 dB and 20 dB, respectively. It can

be seen that the MSE decreases significantly as the number of joint iterations increases and converge to -25 dB as the number of transmitted symbols increases.

It can also be seen that the MSE of the proposed scheme converges to -25 dB (the critical or saturation value) much faster than that of the conventional scheme. More specifically, the JIB_DSICED3 scheme requires only 4 iterations to achieve saturation performance even for a few transmitted symbols while the DSICED3_W/OF scheme remains high error in channel estimation process, e.g. 0 dB for about 10 transmitted symbols in Figures. 3 and 4. Therefore, the proposed JIB_DSICED3 scheme shows its robustness and practical applications in 5G & beyond and IoT transmissions, in which strict requirements of extremely short-packet transmissions and low latency are considered.

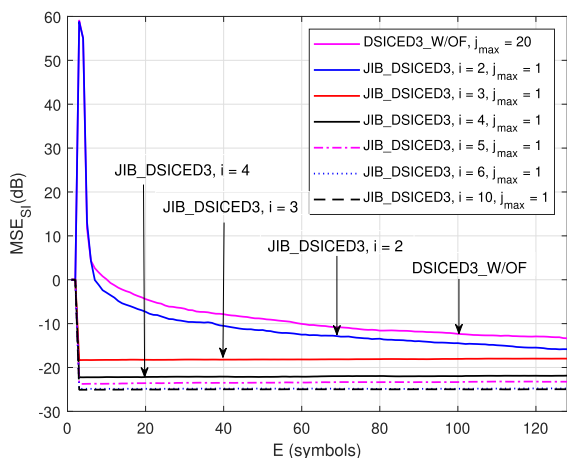


FIGURE 3. MSE_{S_I} (dB) after the i -th decoding iteration versus E symbols; $p_{S_I}/\sigma_w^2 = 30$ dB and $p_B/\sigma_w^2 = 20$ dB.

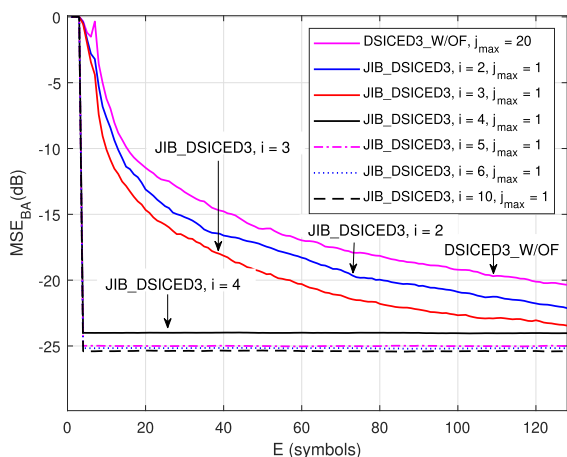


FIGURE 4. MSE_{B_A} (dB) after the i -th decoding iteration versus E symbols; $p_{S_I}/\sigma_w^2 = 30$ dB and $p_B/\sigma_w^2 = 20$ dB.

Fig. 5 and Fig. 6 show the MSE of the SI channel and the intended channel versus the SNR, p_B/σ_w^2 (dB). It can be seen clearly that the MSE decreases as the SNR increases. It can also be observed that the proposed JIB_DSICED3 scheme

outperforms the conventional DSICED3_W/OF scheme, especially for high SNR (≥ 0 dB). The JIB_DSICED3 curves can converge quickly to saturation error floor while the DSICED3_W/OF curves only reach around 10^{-2} to 10^{-3} , although the JIB_DSICED3 scheme needs less iterations than the conventional scheme. The results also show that the blind scheme JIB_DSICED3 is nearly optimal as its performance is approximately reached to that of the lower bound (the BPS scheme), especially in high region of (≥ 0 dB), which is the range of interest in FD transmissions [47].

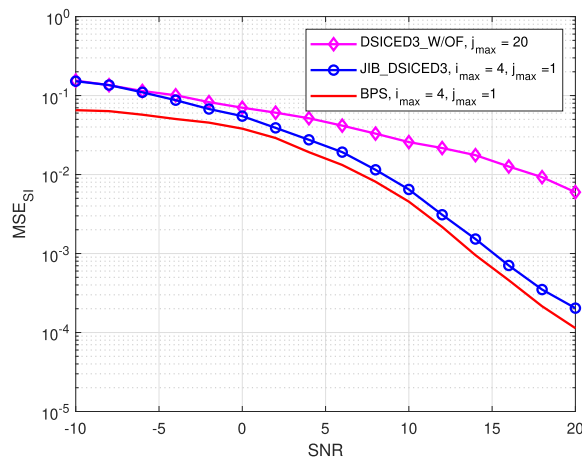


FIGURE 5. MSE_{S_I} versus the SNR, $p_B/\sigma_w^2, p_{S_I}/\sigma_w^2 = 30$ dB and $E = 128$ symbols.

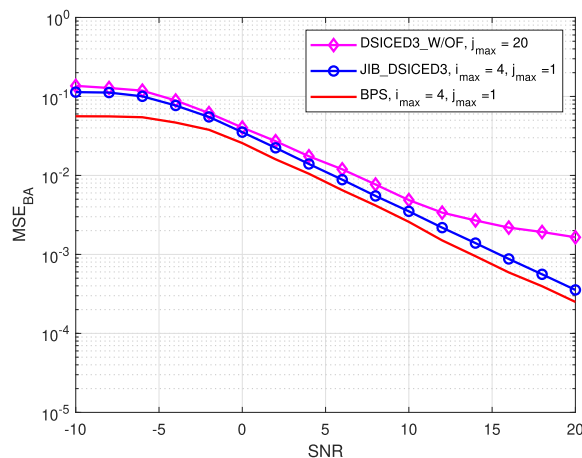


FIGURE 6. MSE_{B_A} versus the SNR, $p_B/\sigma_w^2, p_{S_I}/\sigma_w^2 = 30$ dB and $E = 128$ symbols.

B. BER PERFORMANCES: JIB_DSICED3 VS DSICED3_W/OF

Fig. 7 shows BER of the JIB_DSICED3 scheme after i iterations versus the SNR, p_B/σ_w^2 . It can be seen that BER decreases significantly as the SNR increases and that the gain of JIB_DSICED3 over DSICED3_W/OF is bigger for larger SNR. At low SNR (≤ 0 dB), the conventional DSICED3_W/OF scheme seems to have slightly better in

BER than JIB_DSICED3 scheme. Because the high error of decoding at the first iteration of JIB_DSICED3 scheme in low region of SNR leads to consequence of higher error in next iterations.

However, at high SNR (≥ 0 dB), which is the range of interest in FD transmissions [47], the proposed JIB_DSICED3 scheme outperforms the conventional DSICED3_W/OF scheme even when only 2 iterations are required. Moreover, BER of the proposed JIB_DSICED3 scheme when $i = 4$ is quite closed to that when $i = 10$ and thus, it again confirms the convergence performance when $i = 4$. Moreover, the BER of the proposed JIB_DSICED3 scheme is also closed to that of the lower bound (the BPS scheme), which is obtained by using the best channel estimation of SI channel and intended channel in Fig. 5 and Fig. 6, respectively, for performing SI cancellation and SPA decoding processes with one iterations ($j_{max} = 1$).

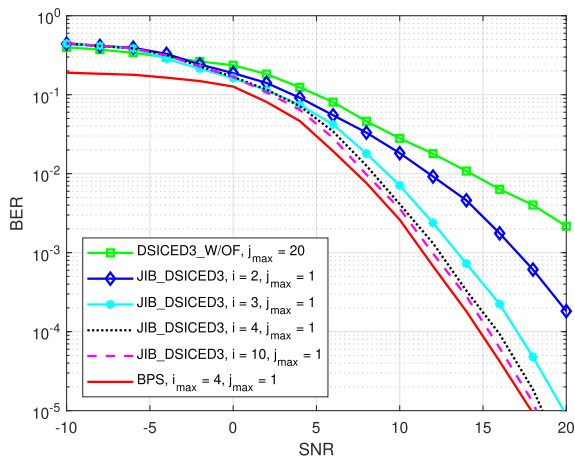


FIGURE 7. BER of JIB_DSICED3 scheme versus the SNR after i iterations, p_B/σ_w^2 for different values of i ; $p_{SI}/\sigma_w^2 = 30$ dB and $E = 128$ symbols.

Fig. 8 shows BER of the proposed JIB_DSICED3 scheme after i iterations versus the SNR, p_B/σ_w^2 , for different values of self-interference to noise ratio, p_{SI}/σ_w^2 . It can be seen that BER increases as the SI power increases and the increase of BER is bigger for larger SNR, p_B/σ_w^2 . Moreover, the result indicates that the increase of SI power has less effects on the proposed JIB_DSICED3 scheme; for example, to maintaining BER at 10^{-4} , it is needed to increase roughly 0.5 dB in the SNR, p_B/σ_w^2 in order to compensate the increasing of 10 dB of self-interference to noise ratio, p_{SI}/σ_w^2 . This result is critical in practical applications since the proposed JIB_DSICED3 scheme is less sensitive to the SI level, which is useful for 5G FD transmission.

IV. PROPOSED JOINT ITERATIVE BLIND PARTIAL FEEDBACK SCHEME VERSION

Although the joint iterative blind scheme JIB_DSICED3 shows its robustness compared to the conventional without feedback scheme DSICED3_W/OF; its processing time still can be improved. In this section, we further introduce a partial

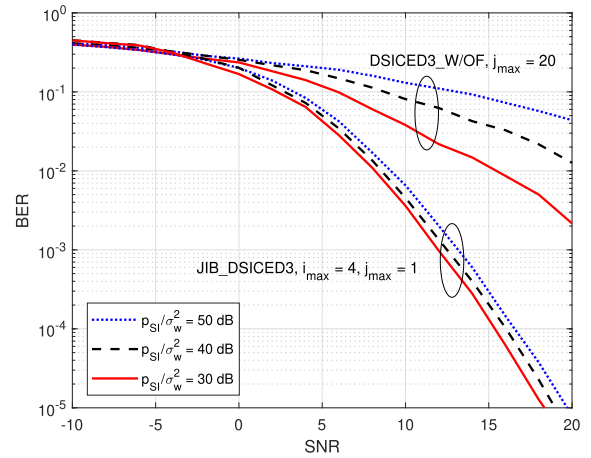


FIGURE 8. BER of JIB_DSICED3 scheme versus the SNR after i iterations, p_B/σ_w^2 , for different value of p_{SI}/σ_w^2 dB; $E = 128$ symbols.

feedback scheme version and name it JIB_DSICED3_PF as Joint Iterative Blind Digital Self-Interference, Equalization, Demodulation, De-interleaving and Decoding with Partial Feedback. Instead of using all modulated symbols for SI channel and intended channel estimation processes in feedback loop, a partial number of modulated symbols αE (with $0 < \alpha \leq 1$), where α is called partial feedback coefficient, will be used to construct the estimation of intended signal and doing subtraction and estimation processes after the first iteration. The *partial feedback* scheme is illustrated in Fig. 9.

Here, the algorithm also performs i_{max} iterations indexed by i for the channel estimation and message decoding. It should be noted that for $i = 1$ (first iteration), a first channel estimation and message decoding is performed to obtain all K bits, which is used to avoid a significant number of errors when starting the process of iterative algorithm. In step 4 of the first iteration, the system perform re-encoded, re-interleaved and re-modulated processes to form E modulated symbols in feedback loop, and only $\alpha E = \alpha N / (\log_2(M))$ symbols is used to form the estimation intended channel and perform updating subtraction and estimation process. From the second iteration $i \geq 2$, the system will perform the channel estimations with partial αE symbols instead of using all symbols, while the decoding process still perform the temporary decoding and feedback loop for all E modulated symbols to get K bits message. When the system reaches the maximum number of iteration i_{max} , the feedback loop is stopped and all symbols are decoded to obtain the estimated binary sequence \hat{x}_{Sol} of node B. The partial feedback algorithm can be summarized in Algorithm 2. Next, we will characterize the performance of the partial feedback scheme JIB_DSICED3_PF in terms of MSE and BER.

A. MSE PERFORMANCES: JIB_DSICED3_PF VS JIB_DSICED3

Fig. 10 and Fig. 11 show the MSE of the SI channel and the intended channel versus number of iterations i for different

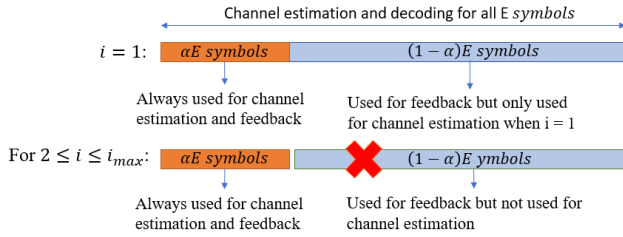


FIGURE 9. Graphical presentation for joint iterative blind partial feedback scheme version.

values of α , respectively and the SNR, $p_B/\sigma_w^2 = 10$ dB, $p_{SI}/\sigma_w^2 = 30$ dB, $E = 128$ symbols. It can be seen that the MSE of the partial feedback scheme JIB_DSICED3_PF converges fast and, when $\alpha K = 32$ symbols or $\alpha = 1/4$, it reaches the saturation performance closed to that of the JIB_DSICED3 scheme. It can also be observed that, when $\alpha E = 32$ symbols or $\alpha = 1/4$, the JIB_DSICED3_PF scheme requires 4 iterations to achieve the saturation performance, similar to the JIB_DSICED3 scheme. Thus, these results indicate the efficient use of partial feedback in both SI and intended channel estimation processes.

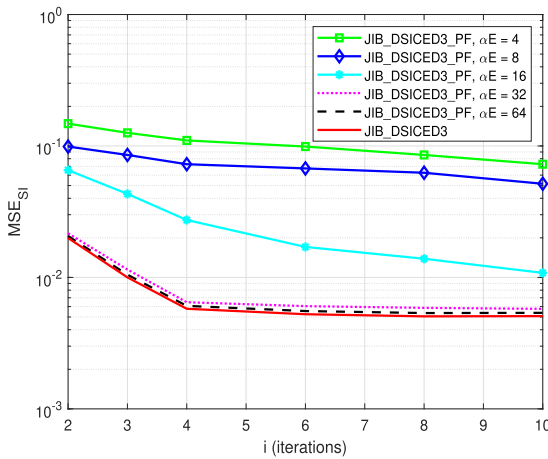


FIGURE 10. MSE_{SI} versus i ; SNR, $p_B/\sigma_w^2 = 10$ dB $p_{SI}/\sigma_w^2 = 30$ dB and $E = 128$ symbols.

B. BER PERFORMANCES: JIB_DSICED3_PF VS JIB_DSICED3

Fig. 12 shows BER of the partial feedback scheme JIB_DSICED3_PF versus α for different value of the SNR, p_B/σ_w^2 . Similar with MSE performances, the BER of JIB_DSICED3_PF scheme also achieves the saturation performance when $\alpha E = 32$ symbols or $\alpha = 1/4$. Furthermore, the comparison of the three schemes such as without feedback DSICED3_W/O/F, with feedback JIB_DSICED3 and with partial feedback JIB_DSICED3_PF, versus total number of modulated symbols, E , is illustrated in Fig. 13. In this case, the different number of information bits $K \in \{32, 64, 128, 256, 512\}$ are used, which correspond to the length of codeword $N \in \{64, 128, 256, 512, 1024\}$ and the

Algorithm 2: Proposed Joint Iterative Blind Partial Feedback Scheme Version

```

Inputs :  $y, x_{SI}, i_{max}, \alpha, K, N, M;$ 
Outputs :  $\hat{h}_{AA}^{(i_{max})}, \hat{h}_{BA}^{(i_{max})}, x_{Sol}^{(i_{max})};$ 
Initialization:  $\hat{y}_{BA}^{(0)} = \mathbf{0}, \hat{h}_{AA}^{(0)} = \mathbf{0}, \hat{h}_{BA}^{(0)} = \mathbf{0}, x_B^{(0)} = \mathbf{0};$ 
for  $i = 1$  to  $i_{max}$  do
  if  $i = 1$  then
    /* Perform Step 1 and Step 2 for all
       of  $E = N/\log_2(M)$  symbols */
    for  $n = 1$  to  $E$  do
      Step 1: SI channel estimation and DSIC process
      Estimate:  $\hat{h}_{AA}^{(i)}$ ;
      Calculate:
       $\tilde{y}^{(i)}[n] = y[n] - \hat{y}_{SI}^{(i)}[n] = y[n] - (\hat{h}_{AA}^{(i)} * x_{SI})[n];$ 
      Step 2: Intended channel estimation
      Estimate:  $\hat{h}_{BA}^{(i)}$  and LLR belief sequence of  $x_{Sol}^{(i)}$ ;
    end
    /* Decoding for all  $K$  bits */
    for  $k = 1$  to  $K$  do
      Step 3: Decoding of the intended signal
      Decoding:  $x_{Sol}^{(i)}[k];$ 
    end
  else
    /* Perform Step 1 and Step 2 for
       only  $\alpha E = \alpha N/(\log_2(M))$  symbols */
    for  $n = 1$  to  $\alpha E$  do
      Step 1: SI channel estimation and DSIC process
      Estimate:  $\hat{h}_{AA}^{(i)}$ ;
      Calculate:
       $\tilde{y}^{(i)}[n] = y[n] - (\hat{h}_{AA}^{(i)} * x_{SI})[n];$ 
      Step 2: Intended channel estimation
      Estimate:  $\hat{h}_{BA}^{(i)}$ ;
    end
    /* Decoding for all  $K$  bits */
    for  $k = 1$  to  $K$  do
      Step 3: Decoding of the intended signal
      Decoding:  $x_{Sol}^{(i)}[k];$ 
    end
  end
  if  $i < i_{max}$  then
    /* Feedback loop with  $E$  symbols */
    for  $n = 1$  to  $E$  do
      Step 4: Feedback loop
      Perform feedback loop to get  $\hat{x}_B^{(i)}$ ;
    end
    /* Updating with only  $\alpha E$  symbols */
    for  $n = 1$  to  $\alpha E$  do
      Calculate:  $\hat{y}_{BA}^{(i)}[n] = (\hat{h}_{BA}^{(i)} * \hat{x}_B^{(i)})[n];$ 
      Update:  $y_{DSIC}^{(i+1)}[n] = y[n] - \hat{y}_{BA}^{(i)}[n];$ 
    end
  else
    /* It is the end of the processing */
    */
    Go to return
  end
end
return  $\hat{h}_{AA}^{(i_{max})}, \hat{h}_{BA}^{(i_{max})}, x_{Sol}^{(i_{max})};$ 

```

length of modulated symbols $E \in \{32, 64, 128, 256, 512\}$, respectively, and the partial feedback coefficient $\alpha = 1/4$. The result shows that the BER performance of JIB_DSICED3

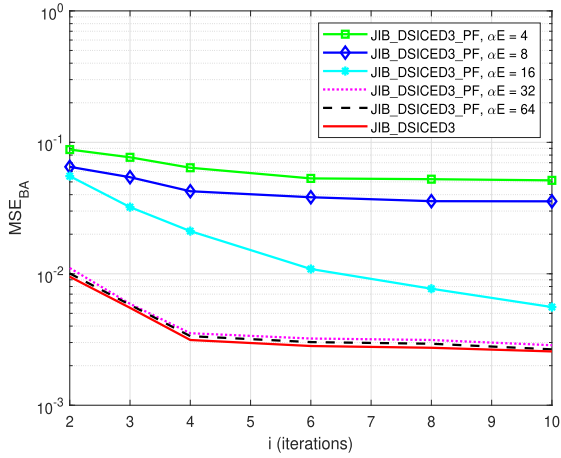


FIGURE 11. MSE_{BA} versus i ; $SNR, p_B/\sigma_w^2 = 10$ dB $p_{SI}/\sigma_w^2 = 30$ dB and $E = 128$ symbols.

and JIB_DSICED3_PF is nearly the same regardless of total number of symbols. Moreover, in low value of SNR, i.e., $SNR = 5$ dB, the two feedback schemes JIB_DSICED3 and JIB_DSICED3_PF also have better performance than the DSICED3_W/OF scheme for small value of E , i.e., $E \leq 128$ symbols and the performance of three schemes converges closed to each other as E is sufficiently large. Furthermore, for larger SNR, i.e., $SNR = 10$ dB, the gap between the two feedback schemes JIB_DSICED3 and JIB_DSICED3_PF compared with the DSICED3_W/OF scheme is also bigger.

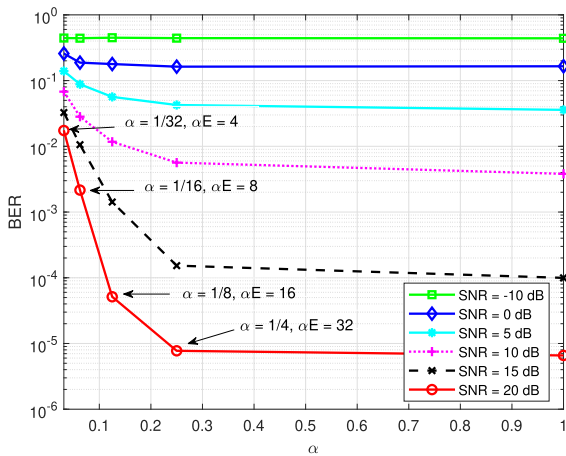


FIGURE 12. BER of JIB_DSICED3_PF scheme versus α ; $i_{max} = 4, j_{max} = 1, p_{SI}/\sigma_w^2 = 30$ dB and $E = 128$ symbols.

Therefore, these results again confirm the efficient use of partial feedback to significantly reduce the computation complexity and processing time, which will be illustrated in Section IV-C, in feedback loop while guaranteeing the close performance of the original with feedback scheme. It also indicates that the two feedback schemes JIB_DSICED3 and JIB_DSICED3_PF are useful for not only short-packet transmission but also for high region of SNR.

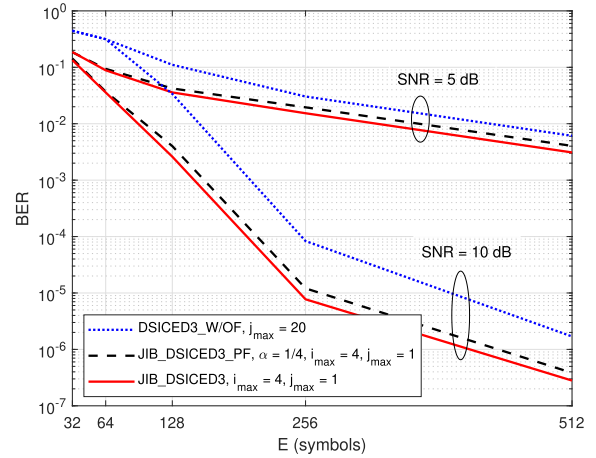


FIGURE 13. BER versus E ; $\alpha = 1/4; p_{SI}/\sigma_w^2 = 30$ dB.

C. COMPARISON OF PROCESSING TIME AND COMPUTATIONAL COMPLEXITY

In this section, we compare the processing time and the computational complexity of the with feedback scheme JIB_DSICED3, partial feedback scheme JIB_DSICED3_PF and the conventional without feedback scheme DSICED3_W/OF. The processing time is a crucial metric for performance evaluation of latency since it quantifies the effectiveness of the algorithm, especially in 5G short-packet transmissions and IoT applications.

A computer with the hardware configuration of Intel (R) Core (TM) I5-10500 CPU @ 3.10 GHz (12 CPUs), memory 16 GB of RAM is used with MATLAB version 2020b. Because the maximum number of decoding iterations is fixed at the same value in order to achieve the optimal (best) results in all cases of SNR, so the processing time for different levels of SNR is nearly the same. Therefore, this configuration is only used to calculate the processing time to obtain the MSE and BER at the particular SNR level, $p_B/\sigma_w^2 = 10$ dB. For the simulation parameters, we set $E = 128$ symbols, $\alpha = 1/4, p_{SI}/\sigma_w^2 = 30$ dB, 10^6 transmission frames, $i_{max} = 4$ and $j_{max} = 1$ for two feedback schemes JIB_DSICED3 and JIB_DSICED3_PF and $j_{max} = 20$ for without feedback scheme DSICED3_W/OF. Based on the results in the Table 3, it can be seen that the with feedback scheme JIB_DSICED3 takes less roughly three times than the without feedback scheme DSICED3_W/OF. This is mainly because of the decreased number of iterations in the SPA decoding, which takes up most of the processing time of the decoder process in 5G QC-LDPC encoded FD short-packet transmissions [27], [28]. Indeed, when $j_{max} = 1$ in two feedback schemes compared with $j_{max} = 20$ in without feedback scheme and these schemes are using the same algorithms for channel estimation (with RLS algorithm) and decoding process (with SPA algorithm).

Furthermore, it is obvious that the processing time is improved in the partial feedback scheme JIB_DSICED3_PF compared to the with feedback scheme JIB_DSICED3 due

to a significant reduce of feedback number of symbols for channel estimation processes (see Figs. 10 and 11 where the partial feedback scheme with $\alpha E = 32$ symbols or $\alpha = 1/4$ requires 4 iterations ($i_{max} = 4$) to achieve the same saturation performance to the with feedback scheme JIB_DSICED3). Thus, nearly two-third or ~ 0.65 times reduce in processing time of the partial feedback scheme JIB_DSICED3_PF is shown in the Table 3.

TABLE 3. Processing Time.

Algorithm	Processing time (in minute)	Ratio respects to (JIB_DSICED3)
DSICED3_W/OF scheme	615.6	1
JIB_DSICED3 scheme	181.2	0.294
JIB_DSICED3_PF scheme	116.8	0.189

Moreover, the computational complexity of three schemes are analyzed based on the summation of the number of computation in operations including additions/subtractions, multiplications/divisions, XOR operation based on [31], [48]–[52]. Because of the identity and symmetric at the transmitter side, this paper only considers to calculate the total number of computations at the receiver side. The formulas for calculating the relative number of computations for each operation are summarized in details in Table. 4, where \bar{d}_v, \bar{d}_c are denoted the average degree of the variable nodes and average degree of the check nodes of parity check matrix \mathbf{H} , respectively.

TABLE 4. Summary of number of computations.

Operation	Number of computations
Modulation/ Demodulation	$\mathcal{O}(N)$
Interleaver/De-Interleaver	$\mathcal{O}(N)$
Encoding	$\mathcal{O}(N)$
SPA decoding	$j_{max} \cdot ((2 \cdot N \cdot \bar{d}_v + (N - K)(3 \cdot \bar{d}_c - 1)))$
RLS algorithm	$\mathcal{O}(E^2)$

Fig. 14 shows the number of computations for different values of symbols E, which is used to calculate the total number of computations to obtain the MSE and BER at the particular SNR level, $p_B/\sigma_w^2 = 10$ dB. For the simulation parameters, we set $\alpha = 1/4$, $p_{SI}/\sigma_w^2 = 30$ dB, 10^6 transmission frames, $i_{max} = 4$ and $j_{max} = 1$ for two feedback schemes JIB_DSICED3 and JIB_DSICED3_PF and $j_{max} = 20$ for without feedback scheme DSICED3_W/OF. It can be seen that the proposed two feedback schemes JIB_DSICED3 and JIB_DSICED3_PF have less cost for completing the computation than the conventional without feedback scheme DSICED3_W/OF.

Therefore, this significant reduce in processing time and computational complexity of the two feedback schemes JIB_DSICED3 and JIB_DSICED3_PF emphasizes the practical implementation of the scheme in 5G short-packet transmissions, especially in IoT transmissions and green communications with low power consumption and low latency.

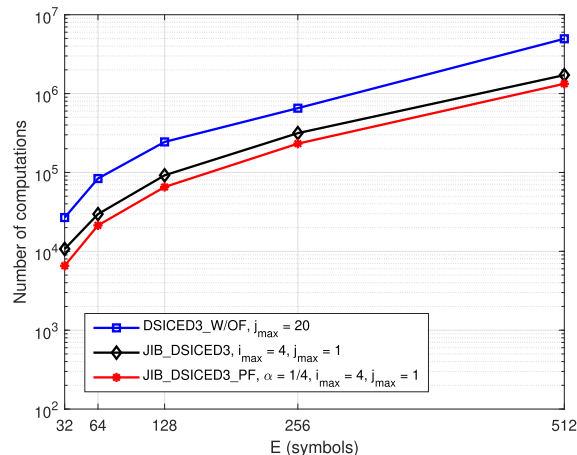


FIGURE 14. Number of computations versus E; $\alpha = 1/4, p_B/\sigma_w^2 = 10$ dB $p_{SI}/\sigma_w^2 = 30$ dB.

V. CONCLUSION

The paper proposed a joint iterative blind channel estimation and decoding algorithm in FD transmissions via feedback of channel estimate and decoded message with DSIC process, named JIB_DSICED3 scheme. The beauty-of-art of the proposed algorithm is taking advantage of iterative algorithms of 5G LDPC at the decoding process to design simultaneous channel estimation and decoding in each iteration in order to efficiently cancel the SI component and improve the simultaneous channel estimation and decoding in the next iteration. To reduce the processing time and computational complexity, the paper further proposed a partial feedback scheme where only a partial number of modulated symbols in feedback loop are used for channel estimations process, named JIB_DSICED3_PF scheme. Numerical results showed that the proposed algorithm outperforms the conventional algorithm DSICED3_W/OF in terms of MSE, BER, processing time and SI sensitivity. More specifically, the proposed algorithm requires only four iterations to achieve the saturation performance and achieve a significant reduce of BER, e.g. about 10^{-1} decrease in BER of the proposed algorithm over the conventional one for the intended SNR of 10 dB. When the self-interference to noise ratio increases 10 dB, the proposed algorithm tends to less sensitive to level of SI as it requires an increasing of 0.5 dB of the intended SNR to maintain the same BER. All these results indicate the practical use of the proposed algorithm in short-packet FD transmissions for IoT applications and green communications with strict requirements of low-latency and energy efficiency. In the near future, a Software Defined Radio (SDR) implementation of the proposed algorithm will be developed in realistic transmission scenarios in order to evaluate its performance on real signals, especially for the error propagation of the channels should be considered and discussed.

REFERENCES

[1] G. Durisi, T. Koch, and P. Popovski, "Toward massive, ultra reliable, and low-Latency wireless communication with short packets," *Proc. IEEE*, vol. 104, no. 9, pp. 1711–1726, Sep. 2016.

- [2] P. Schulz, M. Matthe, H. Klessig, M. Simsek, G. Fettweis, J. Ansari, S. A. Ashraf, B. Almeroth, J. Voigt, I. Riedelet, and A. Puschmann, "Latency critical IoT applications in 5G: Perspective on the design of radio interface and network architecture," *IEEE Commun. Mag.*, vol. 55, no. 2, pp. 70–78, Feb. 2017.
- [3] A. Al-Fuqaha, M. Guizani, M. Mohammadi, M. Aledhari, and M. Ayyash, "Internet of Things: A survey on enabling technologies, protocols, and applications," *IEEE Commun. Surveys Tuts.*, vol. 17, no. 4, pp. 2347–2376, 4th Quart., 2015.
- [4] P. Popovski, "Ultra-reliable communication in 5G wireless systems," in *Proc. 1st Int. Conf. 5G Ubiquitous Connectivity*, 2014, pp. 146–151.
- [5] J. Lee, Y. Kwak, F. Luo, and C. Zhang, "5G standard development: Technology and roadmap," in *Signal Processing for 5G: Algorithms and Implementations* Hoboken, NJ, USA: Wiley, 2016, pp. 561–575.
- [6] C. Bockelmann, N. Pratas, H. Nikopour, K. Au, T. Svensson, C. Ste-fanovic, P. Popovski, and A. Dekorsy, "Massive machine-type communications in 5G: Physical and MAC-layer solutions," *IEEE Commun. Mag.*, vol. 54, no. 9, pp. 59–65, Sep. 2016.
- [7] H.-M. Wang, Q. Yang, Z. Ding, and H. V. Poor, "Secure short-packet communications for mission-critical IoT applications," *IEEE Trans. Wireless Commun.*, vol. 18, no. 5, pp. 2565–2578, May 2019.
- [8] M. Atallah, G. Kaddoum, and L. Kong, "A survey on cooperative jamming applied to physical layer security," in *Proc. IEEE Int. Conf. Ubiquitous Wireless Broadband (ICUWB)*, Oct. 2015, pp. 1–5.
- [9] F. Zhu, F. Gao, T. Zhang, K. Sun, and M. Yao, "Physical-layer security for full duplex communications with self-interference mitigation," *IEEE Trans. Wireless Commun.*, vol. 15, no. 1, pp. 329–340, Jan. 2016.
- [10] S. Hong, J. Brand, J. I. Choi, M. Jain, J. Mehlman, S. Katti, and P. Levis, "Applications of self-interference cancellation in 5G and beyond," *IEEE Commun. Mag.*, vol. 52, no. 2, pp. 114–121, Feb. 2014.
- [11] T. Riihonen, S. Werner, and R. Wichman, "Hybrid full-duplex/half-duplex relaying with transmit power adaptation," *IEEE Trans. Wireless Commun.*, vol. 10, no. 9, pp. 3074–3085, Sep. 2011.
- [12] *Full Duplex Configuration of Un and Uu Subframes for Type I Relay*, document TSG RAN WG1 R1-100139, 3GPP, Jan. 2010.
- [13] *Text Proposal on in Band Full Duplex Relay for TR 36.814*, document TSG RAN WG1 R1-101659, 3GPP, Feb. 2010.
- [14] E. Everett, A. Sahai, and A. Sabharwal, "Passive self-interference suppression for full-duplex infrastructure nodes," *IEEE Trans. Wireless Commun.*, vol. 13, no. 2, pp. 680–694, Jan. 2014.
- [15] C. Anderson, S. Krishnamoorthy, C. Ranson, T. Lemon, W. Newhall, T. Kummertz, and J. Reed, "Antenna isolation, wideband multipath propagation measurements, and interference mitigation for on-frequency repeaters," in *Proc. IEEE Southeast Conf.*, Mar. 2014, pp. 110–114.
- [16] J. I. Choi, S. Hong, M. Jain, S. Katti, P. Levis, and J. Mehlman, "Beyond full duplex wireless," in *Proc. Conf. Rec. 46th Asilomar Conf. Signals, Syst. Comput. (ASILOMAR)*, 2012, pp. 40–44.
- [17] D. Bharadia, E. McMilin, and S. Katti, "Full duplex radios," *ACM SIGCOMM Comput. Commun. Rev.*, vol. 43, no. 4, pp. 375–386, Sep. 2013.
- [18] K. Kolodziej, J. McMichael, and B. Pery, "Adaptive RF canceller for transmit-receive isolation improvement," in *Proc. IEEE Radio Wireless Symp. (RWS)*, Jan. 2014, pp. 172–174.
- [19] E. Ahmed and A. M. Eltawil, "All-digital self-interference cancellation technique for full-duplex systems," *IEEE Trans. Wireless Commun.*, vol. 14, no. 7, pp. 3519–3532, Jul. 2015.
- [20] A. Sabharwal, P. Schniter, D. Guo, D. W. Bliss, S. Rangarajan, and R. Wichman, "In-band full-duplex wireless: Challenges and opportunities," *IEEE J. Sel. Areas Commun.*, vol. 32, no. 9, pp. 1637–1652, Sep. 2014.
- [21] M. Duarte, C. Dick, and A. Sabharwal, "Experiment-driven characterization of full-duplex wireless systems," *IEEE Trans. Wireless Commun.*, vol. 11, no. 12, pp. 4296–4307, Dec. 2012.
- [22] D. Kim, H. Ju, S. Park, and D. Hong, "Effects of channel estimation error on full-duplex two-way networks," *IEEE Trans. Veh. Technol.*, vol. 62, no. 9, pp. 4666–4672, Nov. 2013.
- [23] D. Liu, B. Zhao, F. Wu, S. Shao, X. Pu, and Y. Tang, "Semi-blind SI cancellation for in-band full-duplex wireless communications," *IEEE Commun. Lett.*, vol. 22, no. 5, pp. 1078–1081, May 2018.
- [24] A. Masmoudi and T. Le-Ngoc, "A maximum-likelihood channel estimator for self-interference cancellation in full-duplex systems," *IEEE Trans. Veh. Technol.*, vol. 65, no. 7, 2016.
- [25] A. Masmoudi and T. Le-Ngoc, "Channel estimation and self-interference cancellation in full-duplex communication systems," *IEEE Trans. Veh. Technol.*, vol. 66, no. 1, pp. 5122–5132, Jul. 2017.
- [26] Y. Liu, X. Zhu, E. G. Lim, Y. Jiang, and Y. Huang, "Fast iterative semi-blind receiver for URLLC in short-frame full-duplex systems with CFO," *IEEE J. Sel. Areas Commun.*, vol. 37, no. 4, pp. 839–853, Apr. 2019.
- [27] O. Iscan, D. Lentner, and W. Xu, "A comparison of channel coding schemes for 5G short message transmission," in *Proc. IEEE Globecom Workshops (GC Wkshps)*, Dec. 2016, pp. 1–6.
- [28] Z. R. M. Hajjiyat, A. Sali, M. Mokhtar, and F. Hashim, "Channel coding scheme for 5G mobile communication system for short length message transmission," *Wireless Pers. Commun.*, vol. 106, no. 2, pp. 377–400, May 2019.
- [29] C. Despina-Stoian, A. Digulescu-Popescu, S. Alexandra, R. Youssef, and E. Radoi, "Comparison of adaptive filtering strategies for self-interference cancellation in LTE communication systems," in *Proc. 13th Int. Conf. Commun. (COMM)*, Jun. 2020, pp. 73–76.
- [30] A. T. Kristensen, A. Balatsoukas-Stimming, and A. Burg, "On the implementation complexity of digital full-duplex self-interference cancellation," in *Proc. 54th Asilomar Conf. Signals, Syst., Comput.*, Nov. 2020, pp. 969–973.
- [31] S. Yao, H. Qian, K. Kang, and M. Shen, "A recursive least squares algorithm with reduced complexity for digital predistortion linearization," in *Proc. IEEE Int. Conf. Acoust., Speech Signal Process.*, May 2013, pp. 4736–4739.
- [32] J. H. Bae, A. Abotabl, H.-P. Lin, K.-B. Song, and J. Lee, "An overview of channel coding for 5G NR cellular communications," *APSIPA Trans. Signal Inf. Process.*, vol. 8, no. 17, pp. 1–14, 2019.
- [33] R. G. Gallager, "Low density parity check codes," *IRE Trans. Informat. Theory*, vol. IT-8, no. 1, pp. 21–28, Jan. 1962.
- [34] D. J. C. MacKay, "Good error-correcting codes based on very sparse matrices," *IEEE Trans. Inf. Theory*, vol. 45, no. 2, pp. 399–431, Mar. 1999.
- [35] D. Wang, L. Wang, X. Chen, A. Fei, C. Chen, C. Ju, Z. Wang, and H. Wang, "Construction of irregular QC LDPC codes with low error floor for high speed optical communications," in *Proc. Conf. Lasers Electro-Opt.*, 2016, pp. 1–2.
- [36] X. Zheng, F. C. M. Lau, and T. K. Chi, "Constructing short-length irregular LDPC codes with low error floor," *IEEE Trans. Commun.*, vol. 58, no. 10, pp. 2823–2834, Oct. 2010.
- [37] B. Karimi and A. H. Banihashemi, "Construction of QC LDPC codes with low error floor by efficient systematic search and elimination of trapping sets," *IEEE Trans. Commun.*, vol. 68, no. 2, pp. 697–712, Feb. 2020.
- [38] *Multiplexing and Channel Coding*, document TS 38.212 NR, 3GPP, 2018.
- [39] H. Li, B. Bai, X. Mu, J. Zhang, and H. Xu, "Algebra-assisted construction of quasi-cyclic LDPC codes for 5G new radio," *IEEE Access*, vol. 6, pp. 50229–50244, 2018.
- [40] C. Clapham and J. Nicholson, *The Concise Oxford Dictionary of Mathematics*. Oxford, U.K.: Oxford Univ. Press, 2013.
- [41] E. Sharon, S. Litsyn, and J. Goldberger, "An efficient message-passing schedule for LDPC decoding," in *Proc. IEEE Conv. Electr. Electron. Engineers Isr. Proc.*, Sep. 2004, pp. 223–226.
- [42] X. Zhang and P. H. Siegel, "Quantized iterative message passing decoders with low error floor for LDPC codes," *IEEE Trans. Commun.*, vol. 62, no. 1, pp. 1–14, Jan. 2014.
- [43] B. Q. Vuong, R. Gautier, A. Fiche, and M. Marazin, "Full-duplex efficient channel codes for residual self-interference/quantization noise cancellation," in *Proc. 15th Int. Conf. Signal Process. Commun. Syst. (ICSPCS)*, Dec. 2021, pp. 1–6.
- [44] S. Haykin, *Adaptive Filter Theory*, vol. 29. London, U.K.: Pearson, 1993.
- [45] L. Mostari and A. Taleb-Ahmed, "High performance short-block binary regular LDPC codes," *Alexandria Eng. J.*, vol. 57, no. 4, pp. 2633–2639, Dec. 2018.
- [46] *Guidelines for Evaluation of Radio Transmission Technologies for IMT-2000*, Int. Telecommun. Union, Geneva, Switzerland, 1997.
- [47] V. Aggarwal, M. Duarte, A. Sabharwal, and N. K. Shankaranarayanan, "Full-or half-duplex? A capacity analysis with bounded radio resources," in *Proc. IEEE Inf. Theory Workshop*, Sep. 2012, pp. 207–211.
- [48] I.-D. Ficiu, C.-L. Stanciu, C. Anghel, and C. Elisei-Iliescu, "Low-complexity recursive least-squares adaptive algorithm based on tensorial forms," *Appl. Sci.*, vol. 11, no. 18, p. 8656, Sep. 2021.
- [49] J. K. Kim, S. P. Balakannan, M. H. Lee, and C. J. Kim, "Low complexity encoding of LDPC codes for high-rate and high-speed communication," in *Proc. 1st Int. Conf. Distrib. Framework Appl.*, Oct. 2008, pp. 189–193.
- [50] M. J. Khokhar and M. S. Younis, "Development of the RLS algorithm based on the iterative equation solvers," in *Proc. IEEE 11th Int. Conf. Signal Process.*, Oct. 2012, pp. 272–2753.

- [51] M. Sybis, K. Wesolowski, K. Jayasinghe, V. Venkatasubramanian, and V. Vukadinovic, "Channel coding for ultra-reliable low-latency communication in 5G systems," in *Proc. IEEE 84th Veh. Technol. Conf. (VTC-Fall)*, Sep. 2016, pp. 1–5.
- [52] J. W. Park, D.-S. Yoo, and S.-J. Oh, "Interceptor complexity analysis for mixed BPSK–QPSK modulated frequency hopping spread spectrum systems," *Phys. Commun.*, vol. 40, Jun. 2020, Art. no. 101063.



BAO QUOC VUONG (Graduate Student Member, IEEE) was born in Binh Duong, Vietnam, in December 1992. He received the B.Eng. and M.Eng. degrees in electrical engineering from the School of Electrical Engineering, International University–Vietnam National University–Ho Chi Minh City (IU–VNUHCMC), in 2014 and 2017, respectively. He is currently pursuing the Ph.D. degree with the Information Science and Technology, Communication and Knowledge Laboratory (Lab-STICC), Department of Electrical Engineering, University of Western Brittany, Brest, France. His research interests include the areas of signal processing, wireless communication, information theory, full-duplex transmission, channel coding and cybersecurity for 5G networks, and the Internet of Things.



ROLAND GAUTIER (Member, IEEE) received the M.Sc. degree from the University of Nice Sophia Antipolis, France, in 1995, where his research activities were concerned with the blind source separation of convolutive mixtures for MIMO systems in digital communications, and the Ph.D. degree in electrical engineering from the University of Nice Sophia Antipolis, in 2000, where his research interests were in experiment design for nonlinear parameters models. From 2000 to 2001, he was an Assistant Professor with Polytech-Nantes, Engineering School, University of Nantes, France. Since September 2001, he has been working with the University of Brest, France, as an Associate Professor in electronic engineering and signal processing. From 2007 to June 2012, he was an Assistant Manager of the Laboratory for Science and Technologies of Information, Communication and Knowledge (Lab-STICC—UMR CNRS 6285), Signal Processing Team. From July 2012 to August 2020, he was the Manager of the Defense Research Axis, Lab-STICC, COM Team. His current research interests include the area of signal processing and digital communications, digital communication intelligence (COMINT), analysis, and blind parameters recognition, multiple-access and spread spectrum transmissions, cognitive and software radio, cybersecurity, physical layer security for communications, drones communications detection, and jamming. He received his Habilitation to Supervise Research (HDR) from the University of Brest, in 2013, presenting an overview of his postdoctoral scientific research activities on the development of self-configuring multi-standard adaptive receivers, such as blind analysis of digital transmissions for military communications and cognitive radio. Since 2018, he has been the Holder of the "CyberIoT" Chair of Excellence. Since September 2020, he has been the Manager of the Lab-STIC, Security, Intelligence and Integrity of Information (SI3) Team.



ANTHONY FICHE (Member, IEEE) received the M.S. and Ph.D. degrees from the University of Brest, France, in 2009 and 2012, respectively. Between 2012 and 2014, he was a Postdoctoral Researcher with the Department of Radar and Electro-Magnetic Sensing, ENSTA Bretagne (Lab-STICC UMR CNRS 6285), Brest, where he worked on clutter modeling. Between October 2014 and August 2015, he was a Teaching and Research Temporary Assistant with the University Institute of Technology, Quimper, France. Since September 2015, he has been working with the University of Brest, as an Associate Professor with the Lab-STICC, Team T2I3/SI3. His current research interests include compressed sampling and full duplex communications.



MÉLANIE MARAZIN (Member, IEEE) received the M.Sc. degree in sciences and technologies of telecommunications from the University of Brest, France, in 2006, where her research activities were concerned with the study of performances of a space-time coding on MIMO channel, and the Ph.D. degree in digital communications from the University of Brest, in 2009, where her research interests focus on communications intelligence and blind recognition of convolutional codes. Since 2009, she has been an Assistant Professor with University of Brest. Her general interests lie in the area of signal processing and digital communications. Her current research interests include digital communication interception, analysis, and blind parameters recognition, and the physical layer security for communications. Since 2018, she participates in the "CyberIoT" Chair of Excellence.



HIEN QUANG TA (Member, IEEE) received the bachelor's degree from the Department of Electrical Engineering, Ho Chi Minh University of Technology, in 2010, and the Ph.D. degree from the Department of Electrical and Computer Engineering, Iowa State University, in 2020. He has been with the Faculty of Electrical Engineering, International University (IU)–Vietnam National University, Ho Chi Minh City, Vietnam. Since 2017, he has been a member of IEEE Communication Society (IEEE Comsoc). He received the Graduate Fellowship from Iowa State University, from 2014 to 2020, and the Visiting Graduate Fellowship from Aalborg University, Denmark, in 2018. He also received the Teaching Excellence Award from Iowa State University, in 2017, and the Travel-Grant Scholarship from International and Communication Conference (ICC), Shanghai, China, in 2019. He was served as an Active Reviewer for high-quality peer reviewed journals, such as IEEE COMMUNICATION LETTERS, IEEE TRANSACTIONS ON WIRELESS COMMUNICATIONS, and IEEE INTERNET OF THINGS JOURNAL.



LAP LUAT NGUYEN (Member, IEEE) received the M.Sc. degree in electrical engineering from the International University of Vietnam National University (VNU), Ho Chi Minh City, in 2015, and the Ph.D. degree from the University of Brest (UBO), France, in 2020. Then, he held a teaching and research position at UBO. He is currently a Lecturer at International University, VNU. His research interests include signal processing, wireless communications, and the Internet of Things.